Influence of the excitation threshold of *d* electrons on electronic stopping of slow light ions

D. Goebl, W. Roessler, D. Roth, and P. Bauer*

Institut für Experimentalphysik, Abteilung für Atom- und Oberflächenphysik, Johannes Kepler University Linz, Altenberger Straße 69, 4040 Linz, Austria

(Received 29 January 2014; revised manuscript received 5 June 2014; published 16 October 2014)

We present electronic stopping power data for H and He ions in Zn and In obtained from backscattering experiments in the range of low velocities; for In data are obtained up to the stopping maximum. These results in combination with previous data are analyzed to unravel the influence of *d* electrons in electronic stopping of slow light ions. We report on a systematic difference between the stopping behavior of H and He ions at velocities below 0.2 a.u. Furthermore, we find that the *d*-band offset is not correlated to the velocity at which deviations from velocity proportionality occur. This observation is in contrast to the state-of-the-art models of electronic stopping based on electron-hole pair excitation in a binary Coulomb collision. In this regard we discuss the possible relevance of electron promotion processes in atomic collisions.

DOI: 10.1103/PhysRevA.90.042706 PACS number(s): 34.50.Bw, 34.50.Fa, 73.20.At

I. INTRODUCTION

The process of energy dissipation of slow ions in matter is of great interest not only to manifold applications but also from a fundamental standpoint. The physical quantity, which describes the deceleration processes, is known as the stopping power $S = dE/dx$. By convention, one distinguishes between the electronic stopping power S_e and the nuclear stopping power S_n. Here S_e represents the energy loss to the electronic system, while S_n is due to elastic collisions with target nuclei. To eliminate the dependence of S_e on the number density n of the target, the electronic stopping cross section ε is introduced as $\varepsilon = 1/(nS_e)$.

The physics involved in electronic stopping of light ions is very well understood for high velocities $v \gg v_F$, where v_F denotes the Fermi velocity [1,2]. At ion velocities $v < v_F$, however, there is still a need for a deeper understanding of the prevailing mechanisms. In this regime, the projectiles only interact with weakly bound electrons in the valence or conduction band of the target system. When these electrons are modeled as a free electron gas (FEG), the stopping power is known to be proportional to velocity [3–6],

$$S_e = Q(Z_1, r_s)v \tag{1}$$

Here the friction coefficient Q is a function of the atomic number of the projectile Z_1, and the Wigner-Seitz radius of the FEG, $r_s = (3/4\pi n_e)^{1/3}$, with the FEG density n_e. Since the early days of ion physics, substantial theoretical efforts were devoted to model Q for different projectiles, by use of a variety of approaches to describe the response of the target electrons to the ion charge, e.g., dielectric theory [3,4,7] or density functional theory (DFT) [5,8]. In a thorough analysis of electronic stopping in metals and semiconductors [9], it was demonstrated that Eq. (1) holds for ion velocities up to $v \approx v_F$, and the experimental data are well described by a friction coefficient deduced from the DFT model [5], when the materials are characterized by an effective FEG density, obtained from experimental plasmon losses [10]. Similar success of the DFT model in describing electronic stopping of ions was achieved in grazing scattering geometry, where the interaction is restricted to the electrons in front of the surface [11]. Here one expects a negligible influence of collision induced energy losses and nuclear stopping.

For systems which feature a finite excitation threshold, e.g., *d* bands in noble metals or band gaps in insulators, the stopping power for slow light ions was found to exhibit pronounced deviations from velocity proportionality [12–18]. Similar deviations were also observed for S_e of He in Al [19]; in this case the observed effect was traced back to collision induced electron promotion processes [20].

Recently, electronic stopping of H and He in Pt and Ag had been studied to gain detailed information on the influence of the *d*-band offset E_d on electronic stopping (E_d is given with respect to the Fermi energy E_F; for Pt and Ag, $E_d = 0$ and 4 eV, respectively) [21]. In this study we continue along these lines with an investigation of S_e for H and He ions in Zn and In ($E_d = \sim 8$ and ~ 16 eV, respectively [22]) to obtain further insights into the relevant electronic excitation mechanisms in this regime.

II. EXPERIMENT AND EVALUATION

Experiments were performed in the TOF-LEIS setup ACOLISSA [23]. As samples, evaporated films of In on Si as well as a polished slice from a high-purity Zn rod were used. All samples were sputter cleaned prior to measurement and surface cleanness was checked by Auger electron spectroscopy. After sputtering, AES revealed an oxygen concentration at the surface of ~10%–15% for both samples.

For the metals of interest, the electronic stopping powers were determined relative to a reference material of similar atomic number (Cu and Ag, respectively) by comparison of spectrum heights; to incorporate effects due to nuclear stopping and multiple scattering Monte Carlo simulations were employed using the TRBS code (TRIM for Rutherford backscattering) [24]. In the simulations a Thomas-Fermi-Molière (TFM) potential [25] with a modified Firsov [26] screening length according to O'Connor and Biersack [27] was used. For He scattered from Cu and Zn, a screening length correction factor of 0.75 was applied based on simulations of azimuthal scans [28]. For a detailed description of the

*peter.bauer@jku.at

evaluation procedure, we refer to Ref. [21] where we estimated the precision of this procedure to be within 10%–15% (standard deviation of the statistical uncertainty). The overall systematic error of the deduced values is estimated to be <20%.

In addition to the low velocity regime, the stopping cross section for H and He in In was also determined at velocities up to the stopping maximum, employing the AN700 van de Graaf accelerator at Linz university. For H ions, the evaluation was performed in a similar way to the low-energy case. In relative measurement to Au films, electronic stopping in In is deduced from a comparison of the heights of the leading edges of In and Au. In addition, ε_H and ε_{He} were deduced from backscattering spectra of a double layer Au/In film on a silicon substrate; in this case, the heights at the Au/In interface were evaluated, with the advantage that the beam current does not enter the data analysis. In any case, Monte Carlo simulations were performed to eliminate the influence of multiple scattering on the resulting stopping cross section [24].

In the following we present the data and perform a systematic analysis of band structure effects in metals at low ion velocities. This analysis relies on DFT calculations for H and He in a free electron gas. Numerous studies conducted such calculations, considering different effects at different degrees of complexity [5,8,29–33]. We want to point out that the resulting friction coefficients exhibit qualitatively the same r_s dependence for electron densities corresponding to transition and noble metals, with absolute deviations typically less than 10%. In the present case we have chosen Q_H values [i.e., $Q(Z_1 = 1)$] from [33] and Q_{He} values [i.e., $Q(Z_1 = 2)$] based on [29,32]. Recently, a time-dependent (TD-) DFT study revealed that dynamic many-body exchange-correlation effects become important only for slow ions of intermediate charge [34].

III. RESULTS AND DISCUSSION

In Fig. 1(a) we present the electronic stopping cross section of H in Zn as a function of v; in Fig. 1(b) the corresponding friction coefficient Q is shown [see Eq. (1)], again as a function of v. Results obtained with H^+, H_2^+, and H_3^+ are shown as squares, while data from D^+, D_2^+, and D_3^+ are represented by circles. Consistency is obtained for different isotopes as well as for atomic and molecular ions indicating negligible influence of vicinage or isotope effects. The data exhibit velocity proportionality only for velocities $v < \sim 0.2$ a.u. and $v > \sim 0.5$ a.u., corresponding to proton energies below ~1 and above ~6 keV, respectively, with a smooth transition in the intermediate regime; a line to guide the eye is included. Figure 1 also contains theoretical predictions for $Q_H(r_s)$ calculated by DFT for r_s values of 2.31 and 1.97 a.u. (dash-dotted lines). The r_s value of 2.31 refers to a FEG corresponding to the density of the Zn $4s^2$ electrons, while $r_s = 1.97$ is deduced from experimentally obtained plasmon energies [10], where all conduction electrons contribute. The general agreement between experimental data and the DFT values is very good. Previously measured data for H in Zn obtained in transmission experiments by Martinez-Tamayo *et al.* (MT) [12] are included in Fig. 1(a) (triangles). At our highest velocities, the agreement between our data and the

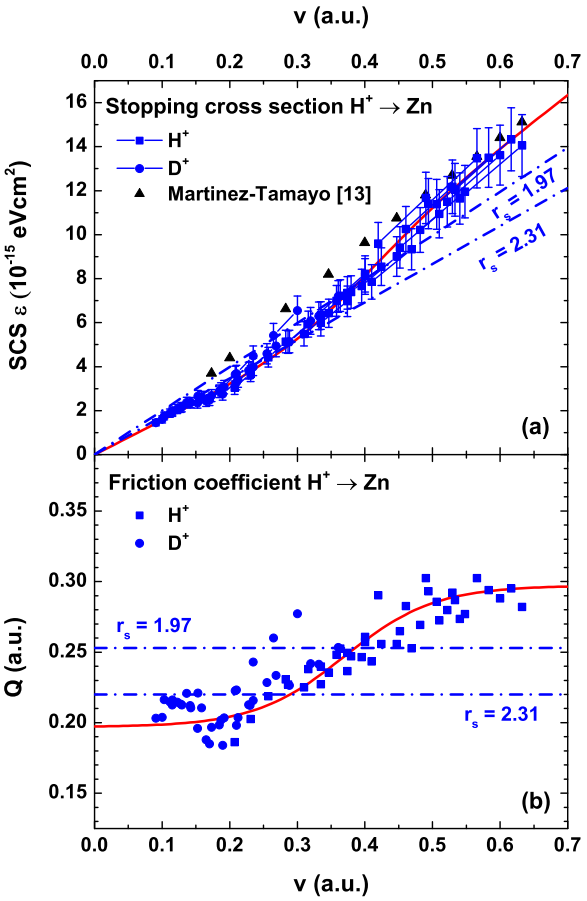

FIG. 1. (Color online) (a) Stopping cross section for elemental and molecular hydrogen (blue squares) and deuterium (blue circles) ions in Zn as a function of ion velocity. Triangles represent previously measured data [13]. Dash-dotted lines indicate results of DFT calculations for different values of r_s. (b) The corresponding friction coefficient Q (in a.u.) is presented as a function of ion velocity. In (a) and (b), the red lines are to guide the eye.

data from [12] is excellent, while at low velocities the MT data exceed ours by ~30%; the transition between the two velocity proportionality regimes is less pronounced for the MT data.

For He^+ ions in Zn our results are shown in Fig. 2 in the same way as for H in Fig. 1. Again, experimental data exhibit velocity proportionality up to ion velocities ~0.2 a.u. For $v > 0.2$ a.u., the friction coefficient increases; at our highest velocity (0.32 a.u.) velocity proportionality is not yet reached again. Figure 2 also contains r_s dependent DFT friction coefficients $Q_{He}(r_s)$ as in Fig. 1. The DFT predictions are in excellent agreement with experimental data at low velocities; for the sake of completeness, the theoretical Q value for $r_s = 1.97$ a.u. is added. Comparison of our data to the experimental data by MT [12] exhibits a striking discrepancy in the whole velocity range: The data from [12] are higher than ours by a factor of 1.6 to 2.4. This is in clear contrast to the good agreement observed for H stopping since in both experiments the same sets of samples were used for H and He projectiles. If the stopping data would systematically depend on the experimental geometry, one would rather expect

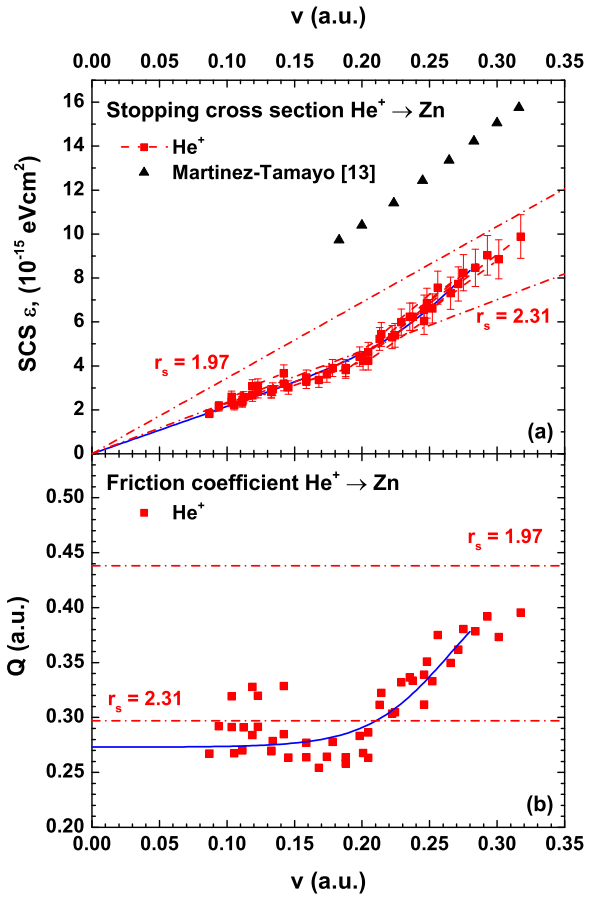

FIG. 2. (Color online) (a) Stopping cross section for He^+ ions in Zn as a function of ion velocity. Our data (red squares) are shown together with theoretical predictions based on DFT for different electron densities (dash-dotted lines). Previously measured data [13] is represented by black triangles. (b) The corresponding friction coefficient Q is shown as a function of ion velocity. In (a) and (b), blue lines are to guide the eye.

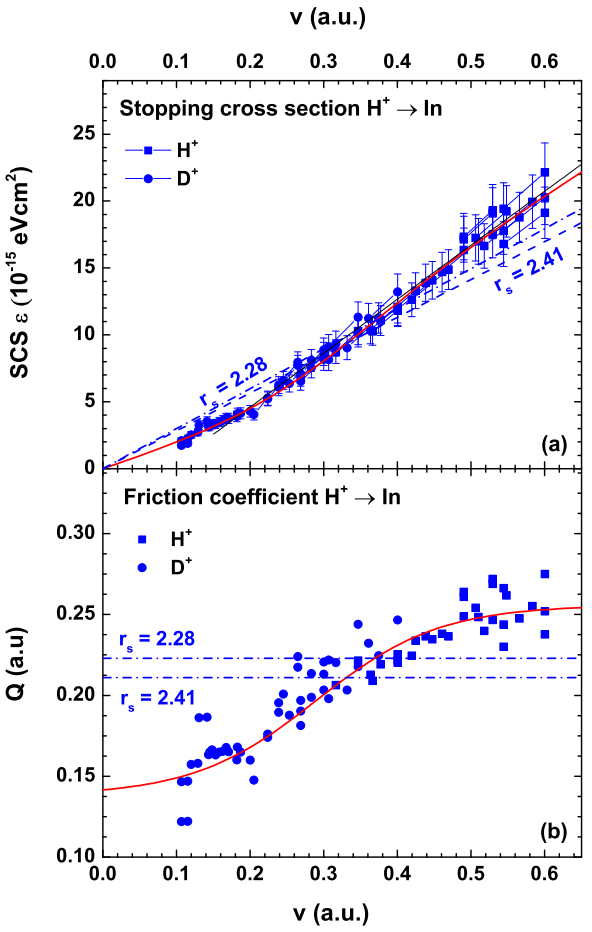

FIG. 3. (Color online) (a) Stopping cross section for H^+ and D^+ ions in In as a function of ion velocity (full squares and full circles, respectively). DFT predictions for electron densities corresponding to r_s values of 2.41 and 2.28, are included in the plot (dash-dotted lines). (b) The corresponding friction coefficient Q is shown as a function of ion velocity. In (a) and (b), red lines are to guide the eye

data from backscattering experiments to be higher, due to possibly enhanced energy loss in collisions with small impact parameters [35]. Thus, the reason for this discrepancy remains unclear. At higher velocities ($v \approx 1.5$ a.u.), the MT data are close to the data by Mertens and Krist [36] (within 20%); also our data extrapolate to these values at higher velocities.

The electronic stopping power of In for H ions and the corresponding friction coefficient are depicted in Figs. 3(a) and 3(b). Data for H (squares) and D (circles), obtained in measurements relative to Ag, are shown. Different isotopes as well as molecular ions result in consistent stopping power data within statistical uncertainty. In the regime $\sim 0.2 < v < \sim 0.5$ a.u., ε data deviate from velocity proportional stopping, as for Zn. The experimental data are compared to predicted $Q_H(r_s)$ values by DFT calculations for a FEG, with $r_s = 2.41$ (according to a $5s^2p^1$ configuration) and $r_s = 2.28$ (deduced from optical data [37]). The absolute values of the DFT results are in fair agreement with our data.

The stopping power data for He^+ in In is presented in Fig. 4(a); in Fig. 4(b) the corresponding friction coefficient data $Q_{He}(r_s)$ are shown as a function of ion velocity. Q values from DFT calculations are presented by dash-dotted lines for the same r_s values as in Fig. 3. For He^+ and In, the experimental data exhibit a velocity proportional behavior up to $v \approx 0.25$ a.u. From the measured data, it is not possible to extrapolate the behavior at $v > 0.32$ a.u.

Additionally, we present the electronic stopping cross section for H and He in In for energies around the stopping maximum in Fig. 5. For H [Fig. 5(a)], data were acquired in relative measurements to a Au film and in direct measurements of a two-layer system (Au/In) on a Si substrate. Both techniques lead to concordant results which are also in good agreement with low velocity data. Figure 5(a) also contains a fit to our low- and high-velocity data (red continuous line), which exhibits minor deviations from the SRIM 2008 [38] curve (dashed line). High velocity data for He were acquired in direct measurements of a two-layer system (Au/In) and are presented in Fig. 5(b) (full squares). In the case of He, the data in both velocity regimes are fairly well described with the SRIM 2008 curve down to 10 keV.

We now discuss the influence of d electrons on electronic stopping, based on the experimental results for Zn and In as

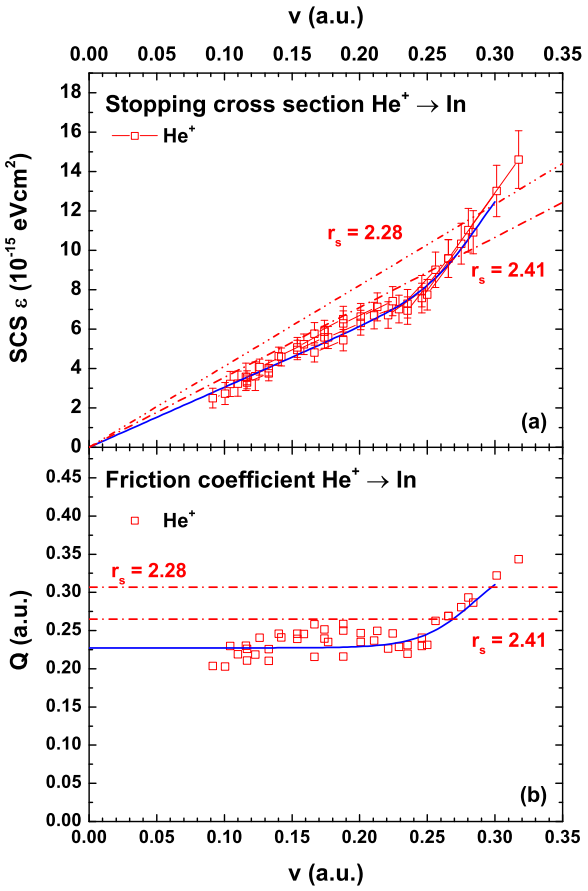

FIG. 4. (Color online) (a) Stopping cross section for He^+ ions in In as a function of ion velocity. Theoretical predictions based on DFT for electron densities $r_s = 2.41$ and $r_s = 2.28$ are included in the plot (dash-dotted lines). (b) The corresponding friction coefficient Q is shown as a function of ion velocity. In (a) and (b), blue lines are to guide the eye.

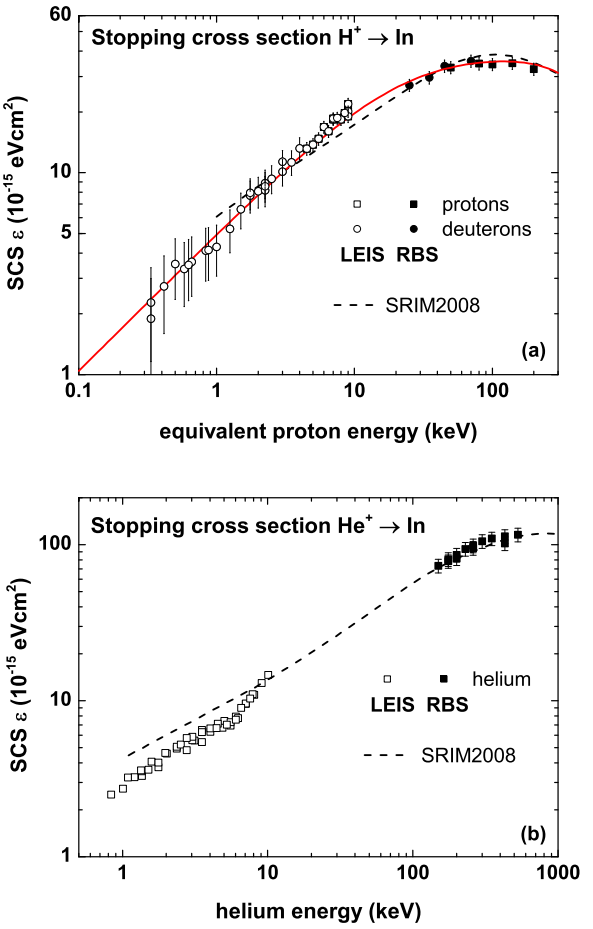

FIG. 5. (Color online) Stopping cross section for protons and deuterons (a) and helium ions (b) in In. Data from Figs. 3 and 4 (open symbols) are shown together with high-velocity data around the stopping maximum (full symbols). Tabulated values from SRIM 2008 are represented by dashed lines. (a) contains a fit of the data in both velocity regimes (red line).

presented above together with other materials with distinct properties of the conduction band (C, Al, Pt, Pd, Cu, Ag, and Au). C and Al do not possess d electrons, for Pt and Pd, the d band reaches up to E_F, while for Cu, Ag, Au, Zn, and In the d bands exhibit excitation thresholds in the range from 2 to 15 eV. Whenever possible we selected data based on backscattering experiments since they do not induce any impact parameter selection [18,19,21], with ε_{H} and $\varepsilon_{\mathrm{He}}$ for C and ε_H for Pd as only exceptions [39,40–42].

To analyze electronic stopping in metals at very low velocities ($v < 0.2$ a.u.) we discuss the r_s dependence of the friction coefficients Q_{H} and Q_{He}, as shown in Fig. 6 for the selected metals. For each material, the experimental values are plotted for two different r_s values. Black squares refer to $r_{s,sp}$ values corresponding to the density of sp electrons in the conduction band, blue diamonds are based on the effective values $r_{s,\mathrm{eff}}$, which adequately describe ε_e at $v \approx v_F$.

When the $r_{s,sp}$ values are employed the r_s dependence of the experimental data is very well described by the DFT model (solid line) in a wide r_s range (1.6 to 3.0 a.u.). The use of $r_{s,\mathrm{eff}}$ leads to excellent agreement only for Pt and Pd, for which the d electrons represent a significant part of the electron density at E_F. This finding can be interpreted in the following way: Unless the d electrons contribute to the density of states at E_F, electronic stopping can be adequately described by using the sp-density only, independent of the d-band offset. The friction coefficient obtained in TD-DFT calculations for channeled ions in gold (red asterisk) [43] is low compared to our data, probably due to the low electron density in channeling conditions. Thus, for slow H ions ($v < 0.2$ a.u.) excitation of sp electrons is the dominant mechanism in electronic stopping in metals; excitation of d electrons only plays a role if the d band extends up to E_F.

Figure 7 displays the equivalent information for He ions. As for H, stopping for C, Al, Zn, and In is very well described by the FEG theory when using $r_{s,sp}$ (black squares); for Pt, the use of $r_{s,\mathrm{eff}}$ (blue diamonds) is appropriate. For noble metals the Q_{He} data exhibit an r_s dependence different from that of the DFT predictions: When presented as a function of $r_{s,sp}$ the experimental data are high by up to a factor of ~2.5 and they are low by up to a factor of ~3 when $r_{s,\mathrm{eff}}$ is used. Also for He the TD-DFT data (asterisk) are low compared to our data, probably for the same reason as for H ions [43].

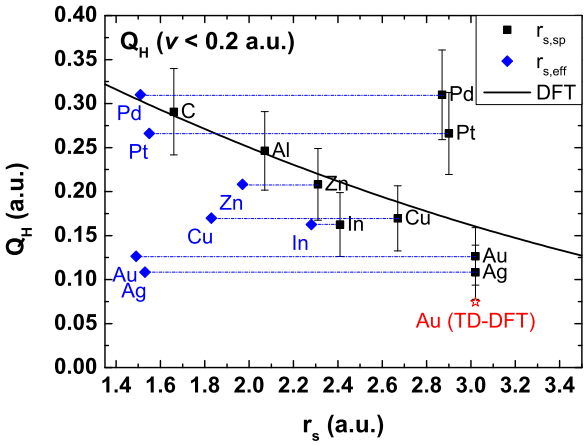

FIG. 6. (Color online) Experimental friction coefficients for H ions Q_{H} as a function of r_s, at $v < 0.2$ a.u. Black squares correspond to $r_{s,sp}$ values based on sp electrons only, blue diamonds represent effective $r_{s,\mathrm{eff}}$ values based on experimental plasmon energies [10]. The solid line indicates the friction coefficient predicted by DFT calculations. The asterisk corresponds to data obtained in TD-DFT calculations [43]. For Pt and Pd, $r_{s,sp}$ was calculated assuming a single s electron.

In [43] it was deduced that for Au the ratio $Q_{\mathrm{He}}/Q_{\mathrm{H}}$ exceeds predictions for $r_{s,sp}$ due to an enhanced participation of d electrons in the interaction with He. Our experimental data suggest that this is true for all noble metals.

In a next step we want to investigate to which extent Q_{He} is influenced by the d-band excitation threshold E_d. To this end, we present the ratio $Q_{\mathrm{He}}^{\mathrm{expt}}/Q_{\mathrm{He}}^{\mathrm{FEG},sp}$ as a function of E_d in Fig. 8. This ratio clearly follows a trend: The relative importance of d excitation is largest for $E_d = 2$ eV and decreases with increasing E_d, until it vanishes for $E_d \geqslant 8$ eV. This is a strong indication that for He ions excitation of d electrons is already possible

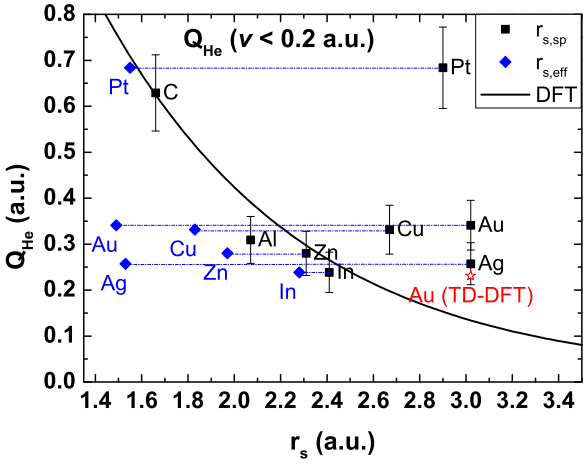

FIG. 7. (Color online) Experimental friction coefficients for He ions Q_{He} as a function of r_s. Black squares refer to $r_{s,sp}$ values based on sp electrons only, the blue diamonds represent effective $r_{s,\mathrm{eff}}$ values deduced from experimental plasmon energies [10]. The solid line indicates the friction coefficient predicted by DFT calculations. The red asterisk corresponds to data obtained in TD-DFT calculations [43]. For Pt, a single s electron was assumed when calculating $r_{s,sp}$.

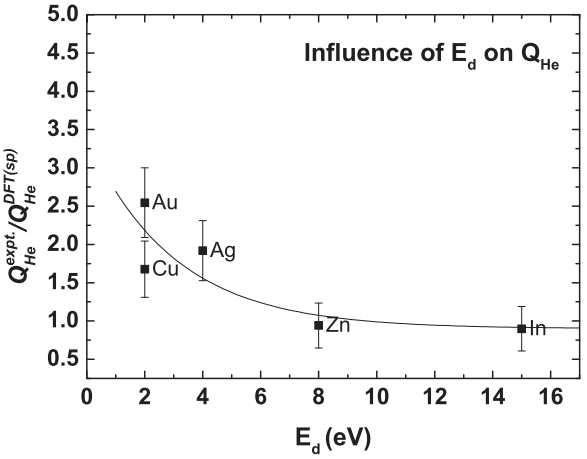

FIG. 8. Friction coefficient ratio for He ions as a function of the d-band offset E_d. Solid line is to guide the eye.

at ion velocities $v < 0.2$ a.u. (4 keV He) for $E_d \leqslant 8$ eV. Cu and Au exhibit nearly identical excitation thresholds, but for Au Q_{He} is slightly higher than for Cu despite the fact that Cu exhibits a higher sp density than gold. This points toward the fact that other properties like the spatial distribution of the electrons may have a significant influence on the friction coefficient.

To complete the picture for $v < 0.2$, we present the corresponding $Q_{\mathrm{He}}/Q_{\mathrm{H}}$ values in Fig. 9 together with predictions by DFT calculations. Again, experimental values are given for both $r_{s,sp}$ (black squares) and $r_{s,\mathrm{eff}}$ (blue diamonds), respectively. Since electronic stopping of He in the noble metals is not adequately described by theory, for $Q_{\mathrm{He}}/Q_{\mathrm{H}}$ a large mismatch between DFT predictions and experimental values is expected. Surprisingly, perfect agreement is achieved, when the data are presented as a function of $r_{s,\mathrm{eff}}$, despite the fact that for both Q_{H} and Q_{He}, the theoretical values exceed the experimental ones by a factor of $\sim$3 as shown in Figs. 6 and 7. Whether this finding is fortuitous or due to unknown physical reasons is unclear.

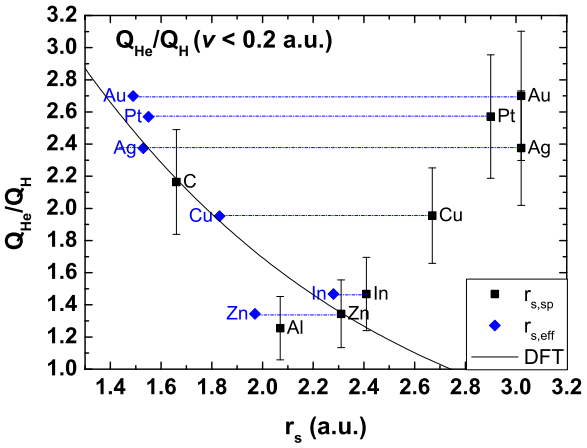

FIG. 9. (Color online) Friction coefficient ratio $Q_{\mathrm{He}}/Q_{\mathrm{H}}$ as a function of r_s. Data are presented as a function of $r_{s,sp}$ (black squares) and $r_{s,\mathrm{eff}}$ (blue diamonds), respectively. The predicted values according to DFT calculations are indicated by the solid line.

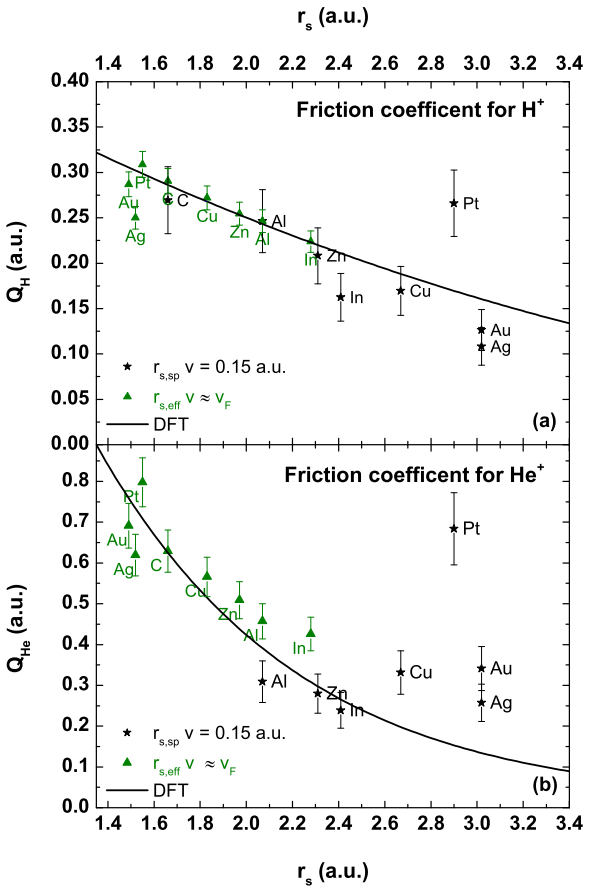

FIG. 10. (Color online) Experimental friction coefficients for H (a) and He (b) ions in different materials as a function of r_s. Data are shown for $v = 0.15$ a.u., where the density of the FEG is based on sp-electrons only (asterisks) and for $v \approx v_F$, where $r_{s,\mathrm{eff}}$ is employed which is based on experimental plasmon energies (green triangles). For H, data are taken from Al [19,45], Ag [21,46,47], Au [18,48], C [41,49,50], Cu [18,51,52], Pt [21,48], Zn [53,54]. For He, data are taken from Al [19,55], Ag [21,47], Au [18,48], C [39,40], Cu [18,51], Pt [21,48], Zn [54].

We now continue with an evaluation of Q_{H} and Q_{He} at higher velocities. The regime of velocities below 0.2 a.u. has been discussed above, while the regime $v \approx v_F$ has been investigated in detail in Refs. [9] and [44]. To combine these two regimes we present friction coefficients Q_{H} and Q_{He} for H and He ions, respectively, as a function of r_s [see Figs. 10(a) and 10(b)]. We depict experimental data obtained at $v = 0.15$ a.u. and at $v \approx v_F$ as a function of $r_{s,sp}$ and of $r_{s,\mathrm{eff}}$, respectively. In this way of representation, the data are very well described by the theoretical values based on DFT calculations, with the exceptions (H-Pt, He-Pt, and He-noble metals) as discussed above.

As a next step we connect the observed features of ε_{H} and of $\varepsilon_{\mathrm{He}}$ to the d-band offsets of the metals. In previous studies, the observed deviations from velocity proportionality were characterized by so-called kink velocities v_k, which were obtained as intersects of linear fits to the low velocity regime where $\varepsilon \propto v$ holds, and to the transition regime where $\varepsilon \propto (v - v_{\mathrm{offset}})$ [18]. These kink velocities were interpreted as a consequence of band structure effects (onset of d-band excitations), assuming a maximum energy transfer in a binary collision between an ion and an electron, $\Delta E_{\max} = 2v_{\mathrm{k}}v_{\mathrm{F}} = E_d$ [3,15–17,56]. Table I presents the kink velocities v_k for H and He ions in different materials. In addition, the ratio $R = Q_{\mathrm{expt}}(v \approx v_F)/Q_{\mathrm{expt}}(v = 0.15$ a.u.) is shown for H and He ions. R measures how much the slopes of electronic stopping differ at $v = 0.15$ a.u. and $v \approx v_F$; $R = 1$ refers to the case of $Q =$ const in the velocity regime $0 < v < v_{\mathrm{F}}$. Finally, Table I contains the ratio $R_{\mathrm{He}}/R_{\mathrm{H}}$ which measures whether Q_{H} and Q_{He} behave differently in the transition regime. $R_{\mathrm{He}}/R_{\mathrm{H}} = 1$ corresponds to equivalent behavior of ε_{H} and $\varepsilon_{\mathrm{He}}$ in the transition regime, significant deviations from unity point to different dominant energy loss mechanisms for H and He.

TABLE I. Overview over d-band offsets E_d [57,58], kink-velocities v_k, friction coefficient ratios $R = Q_{\mathrm{expt}}(v = v_F)/Q_{\mathrm{expt}}(v = 0.15$ a.u.) for H and He ions and the ratio $R_{\mathrm{He}}/R_{\mathrm{H}}$.

Material	E_d (eV)	v_k (a.u.) - H	R_{H}	v_k (a.u.) - He	R_{He}	$R_{\mathrm{He}}/R_{\mathrm{H}}$
Al	–	–	1.0	0.2	1.48	1.48
Pt	0	–	1.16	0.17	1.16	1.00
Cu	2	0.18	1.62	0.19	1.71	1.06
Au	2	0.19	2.26	0.19	2.03	0.90
Ag	4	0.20	2.32	0.19	2.40	1.03
Zn	8	0.21	1.22	0.20	1.81	1.48
In	15	0.19	1.37	0.25	1.93	1.41

We now focus on the transition region where electronic stopping is not velocity proportional, i.e., for $0.2 < v < \sim 0.6$ a.u. In this regime there is still a lack of understanding of the relevant physical processes. The fact that data for Q_{H} show excellent agreement to theory for $v < 0.2$ a.u. *and* for $v \approx v_F$ implies for materials with $r_{s,sp} \neq r_{s,\mathrm{eff}}$ that $R_{\mathrm{H}} > 1$, i.e., Q must change at intermediate velocities. As one can see in Table I, R_{H} is close to 1 for Al and Pt ($E_d = 0$) as well as for Zn and In, where $E_d \geqslant 8$ eV and exhibits a maximum for the noble metals ($E_d = 2$ to 4 eV). Electron-hole pair excitation in a binary encounter ($\Delta E_{\max} = 2vv_F$) cannot explain why the range of v_k values is very limited (0.18 to 0.21 a.u.), despite considerable variations in E_d (0 to 15 eV). Existing data indicate that for H projectiles deviations from velocity proportionality occur only for a small number of materials with a fully occupied d band in the vicinity or above the unperturbed H-1s level. If the d band is significantly below the unperturbed H-1s level, e.g., for H in Ge, no deviations from velocity proportionality are observed [59].

A possible process, which might explain the unresolved observations, is inelastic energy loss in atomic collisions due to electron promotion. This mechanism has been extensively studied for a large variety of projectile-surface combinations [20,60–69]. In a close encounter, the electronic energy levels of the projectile and target atom shift due to the formation of a quasimolecule. Depending on the projectile-target combination and the scattering conditions, charge exchange and/or electronic excitations may occur. Aono and Souda, e.g., identified an energy loss of ~20 eV for He projectiles which were subject to Auger neutralization and subsequently reionized in a close collision [20]; Esaulov *et al.* reported on excitations of He to the $2s^2$ state in collisions with an Al target [61].

For a quantitative evaluation, one has to consider the scattering angle distribution and the corresponding cross sections for these processes to be able to relate these findings for single scattering collisions to our energy loss experiments. For instance, experiments for Al were conducted in so-called "double-transmission" geometry, where the shift of the high energy edge was evaluated for projectiles backscattered from clean Ta and Ta covered with a thin layer of Al. In this specific geometry, projectiles which experience a large angle scattering event with an Al atom exhibit a large elastic energy transfer and consequently do not contribute to the evaluation [70]. Also in "conventional" backscattering experiments, such as presented in this investigation, large impact parameters prevail [35]. If an identical energy loss occurs in the backscattering event for every trajectory, we would simply observe a constant shift of our spectra, which would not influence the evaluated stopping power. In that sense we do not think that one should expect large differences in the magnitude of ε for different scattering geometries. One should expect that a collision induced energy loss process can significantly contribute to the stopping power at low velocities only if it occurs at a rather large impact parameter. For instance, the reionization process for He or Al is possible at an energy as low as ~200 eV in a binary collision with a scattering angle $\geqslant 129°$ [71]; a significant contribution of this process to the inelastic energy loss, however, can be found at much higher primary energies ($\geqslant \sim 4$ keV [19,70]). Zn and In show a similar behaviour of electronic stopping as Al: The deviation from velocity proportionality for He is significantly stronger than for H ($R_{\mathrm{He}}/R_{\mathrm{H}} > 1.4$, see Table I). We attribute this behavior to different mechanisms that are active for He but not for H. Note that any collision induced excitation processes may contribute to electronic stopping—charge exchange or excitation of target electrons, as observed for He and different target materials [20]. On this basis the stopping behavior of He in In and Zn may fit into the picture despite their comparatively high thresholds of reionization [20].

Here we want to add a short discussion concerning the efficiency of the above mentioned promotion processes. Aono and Souda have observed that the threshold energy for reionization increases with increasing group and period in the periodic system of elements [20]. One may expect that for a given energy, the efficiency of this process is larger for materials with a lower threshold energy, but accurate numbers are very scarce (Hartree-Fock calculations, as performed in [72], only lead to qualitative results). Quantitative quantum chemistry calculations have been performed only for a few selected systems and here only for specific geometries [73].

An interesting question, which is related to the processes discussed above, is the one about the charge state of the intruder when moving in a metal. This question is more relevant for He, since H is expected to feature no bound states within a conductor [74]. In contrast, in DFT calculations, which are used to determine the friction coefficients, two bound electrons can be attributed to the H projectile. Interestingly, explicit calculations of electronic stopping considering bound electrons and stripped projectiles did not reveal significantly different results [75]. Consequently, from comparison of experimental data to DFT calculations one cannot decide on the existence of electron states bound to a proton in a metal. Note that when various charge states are possible, the resulting stopping comprises both, charge state dependent contributions for each of the charge fractions and the energy loss in a full charge exchange cycle [76].

In any case, a definite answer about the role of collision induced energy loss processes in electronic stopping can only be given after thorough theoretical treatment of this subject. In that sense we would hope that these results will stimulate further research along these lines.

IV. CONCLUSION

We have presented electronic stopping cross section data of Zn and In for slow hydrogen, deuterium, and helium ions, obtained from backscattering experiments. In addition, for In the energy range was extended up to the stopping maximum due to a lack of available data.

To gain further insight in electronic stopping we compared the results to available stopping power data for different transition and noble metals. At velocities $v \leqslant v_F$, two distinct regimes of velocity proportional stopping are observed, i.e., at $v < 0.2$ a.u. and at $v \approx v_F$. In both regimes, dE/dx can be described by a FEG-based DFT theory when using appropriate electron densities.

For $v < 0.2$ a.u. we revealed a systematic difference in the role of d bands in electronic stopping of H and He ions in metals. For H, the d-band participates in the stopping process only if it extends up to E_F; even Cu and Au can be adequately described by a DFT model which considers sp electrons only. In contrast, He can excite deeper lying d electrons, at least up to $E_d \approx 4$ eV. Stopping in metals which exhibit a significant contribution of d electrons to the DOS at E_F can be adequately described using an effective electron density obtained from experimental plasmon energies. The concept of an effective electron density is also suitable to describe electronic stopping at $v \approx v_F$, leading to excellent agreement between theory and experiment.

The onset of the transition regime, i.e., the so-called kink velocity, was found to be rather independent of the detailed properties of the d band. This finding is not compatible with electron-hole pair excitation in a Coulomb collision [3], but may instead be traced back to energy loss due to electron promotion in atomic collisions, e.g., in re-ionizing collisions. Further clarification of these observations definitely requires a thorough theoretical investigation.

ACKNOWLEDGMENTS

Support by the Austrian Science Fund (FWF): Project P22587 is gratefully acknowledged. Dominik Goebl was supported by a DOC fellowship of the Austrian Academy of Sciences.

[1] C. P. Race, D. R. Mason, M. W. Finnis, W. M. C. Foulkes, A. P. Horsfield, and A. P. Sutton, Rep. Prog. Phys. **73**, 116501 (2010).

[2] P. Sigmund, *Particle Penetration and Radiation Effects General Aspects and Stopping of Swift Point Charges* (Springer, Berlin, 2008).

[3] E. Fermi and E. Teller, Phys. Rev. **72**, 399 (1947).
[4] J. Lindhard, Mat. Fys. Medd. Dan. Vid. Selsk. **28**, 8 (1954).
[5] P. M. Echenique, R. M. Nieminen, and R. H. Ritchie, Solid State Commun. **37**, 779 (1981).
[6] S. P. Møller, A. Csete, T. Ichioka, H. Knudsen, U. I. Uggerhøj, and H. H. Andersen, Phys. Rev. Lett. **93**, 042502 (2004).
[7] R. H. Ritchie, Phys. Rev. **114**, 644 (1959).
[8] I. Nagy, A. Arnau, and P. M. Echenique, Phys. Rev. A **40**, 987 (1989).
[9] A. Mann and W. Brandt, Phys. Rev. B **24**, 4999 (1981).
[10] D. Isaakson, *Compilation of rs Values*, New York University Doc. No. 02698 (National Auxiliary Publication Service, New York, 1975).
[11] H. Winter, Phys. Rep. **367**, 387 (2002).
[12] J. E. Valdés, J. C. Eckardt, G. H. Lantschner, and N. R. Arista, Phys. Rev. A **49**, 1083 (1994).
[13] G. Martínez-Tamayo, J. C. Eckardt, G. H. Lantschner, and N. R. Arista, Phys. Rev. A **54**, 3131 (1996).
[14] E. A. Figueroa, E. D. Cantero, J. C. Eckardt, G. H. Lantschner, J. E. Valdés, and N. R. Arista, Phys. Rev. A **75**, 010901(R) (2007).
[15] E. A. Figueroa, E. D. Cantero, J. C. Eckardt, G. H. Lantschner, and N. R. Arista, Phys. Rev. A **75**, 064902 (2007).
[16] S. N. Markin, D. Primetzhofer, S. Prusa, M. Brunmayr, G. Kowarik, F. Aumayr, and P. Bauer, Phys. Rev. B **78**, 195122 (2008).
[17] E. D. Cantero, G. H. Lantschner, J. C. Eckardt, and N. R. Arista, Phys. Rev. A **80**, 032904 (2009).
[18] S. N. Markin, D. Primetzhofer, M. Spitz, and P. Bauer, Phys. Rev. B **80**, 205105 (2009).
[19] D. Primetzhofer, S. Rund, D. Roth, D. Goebl, and P. Bauer, Phys. Rev. Lett. **107**, 163201 (2011).
[20] M. Aono and R. Souda, Nucl. Instrum. Method Phys. Res. B **27**, 55 (1987).
[21] D. Goebl, D. Roth, and P. Bauer, Phys. Rev. A **87**, 062903 (2013).
[22] R. T. Poole, P. C. Kemeny, J. Liesegang, J. G. Jenkin, and R. C. G. Leckey, J. Phys. F: Met. Phys. **3**, L46 (1973).
[23] M. Draxler, S. N. Markin, S. N. Ermolov, K. Schmid, C. Hesch, A. Poschacher, R. Gruber, M Bergsmann, and P. Bauer, Vacuum **73**, 39 (2004).
[24] J. P. Biersack, E. Steinbauer, and P. Bauer, Nucl. Instrum. Method Phys. Res. B **61**, 77 (1991).
[25] G. Molière, Z. Naturforsch. A **2**, 133 (1947).
[26] O. B. Firsov, Sov. Phys. JETP-USSR **6**, 534 (1958).
[27] D. J. O'Connor and J. P. Biersack, Nucl. Instrum. Method Phys. Res. B **15**, 14 (1986).
[28] D. Primetzhofer, S. N. Markin, M. Draxler, R. Beikler, E. Taglauer, and P. Bauer, Surf. Sci. **602**, 2921 (2008).
[29] M. J. Puska and R. M. Nieminen, Phys. Rev. B **27**, 6121 (1983).
[30] P. M. Echenique, R. M. Nieminen, J. C. Ashley, and R. H. Ritchie, Phys. Rev. A **33**, 897 (1986).
[31] P. M. Echenique, A. Arnau, M. Penalba, and I. Nagy, Nucl. Instrum. Method Phys. Res. B **56-57**, 345 (1991).
[32] I. Nagy and A. Arnau, Phys. Rev. B **49**, 9955 (1994).
[33] J. I. Juaristi, M. Alducin, R. Díez Muiño, H. F. Busnengo, and A. Salin, Phys. Rev. Lett. **100**, 116102 (2008).
[34] V. U. Nazarov, J. M. Pitarke, C. S. Kim, and Y. Takada, Phys. Rev. B **71**, 121106 (2005).
[35] D. Goebl, K. Khalal-Kouache, D. Roth, E. Steinbauerm and P. Bauer, Phys. Rev. A **88**, 032901 (2013).
[36] P. Mertens and Th. Krist, J. Appl. Phys. **53**, 7343 (1982).
[37] R. Y. Koyama, N. V. Smith, and W. E. Spicer, Phys. Rev. B **8**, 2426 (1973).
[38] J. F. Ziegler, J. P. Biersack, and M. D. Ziegler, "SRIM-2008 software package" available online at http://www.srim.org.
[39] A. van Wijngaarden and H. E. Duckworth, Can. J. Phys. **40**, 1749 (1962).
[40] J. H. Ormrod and H. E. Duckworth, Can. J. Phys. **41**, 1424 (1963).
[41] R. Golser, Ch. Eppacher, and D. Semrad, Nucl. Instrum. Method Phys. Res. B **67**, 69 (1992).
[42] C. Celedón, E. A. Sánchez, M. S. Moreno, N. R. Arista, J. D. Uribe, M. Mery, J. E. Valdés, and P. Vargas, Phys. Rev. A **88**, 012903 (2013).
[43] M. A. Zeb, J. Kohanoff, D. Sánchez-Portal, A. Arnau, J. I. Juaristi, and E. Artacho, Phys. Rev. Lett. **108**, 225504 (2012).
[44] I. Nagy, Ch. Eppacher, and D. Semrad, Phys. Rev. B **62**, 5270 (2000).
[45] J. E. Valdés, G. Martínez-Tamayo, G. H. Lantschner, J. C. Eckardt, and N. R. Arista, Nucl. Instrum. Method Phys. Res. B **73**, 313 (1993).
[46] Ch. Eppacher and D. Semrad, Nucl. Instrum. Method Phys. Res. B **69**, 33 (1992).
[47] Ch. Eppacher, Ph.D. Thesis, Univ. Linz, Schriften der Johannes Kepler Universität, Universitätsverlag Rudolf Trauner, 1995.
[48] D. Primetzhofer, Phys. Rev. B **86**, 094102 (2012).
[49] S. H. Overbury, P. F. Dittner, S. Datz, and R. S. Thoe, Radiat. Effects **41**, 219 (1979).
[50] E. P. Arkhipov and Yu. V. Gott, Sov. Phys. JETP-USSR **29**, 615 (1969).
[51] D. Semrad, P. Bauer, F. Aumayr, P. Huber, and W. Obermann, Nucl. Instrum. Method Phys. Res. **218**, 811 (1983).
[52] W. White and R. M. Mueller, Phys. Rev. **187**, 499 (1969).
[53] P. Bauer, F. Kastner, A. Arnau, A. Salin, P. D. Fainstein, V. H. Ponce, and P. M. Echenique, Phys. Rev. Lett. **69**, 1137 (1992).
[54] G. Martínez-Tamayo, J. C. Eckardt, G. H. Lantschner, and N. R. Arista, Phys. Rev. A **51**, 2285 (1995).
[55] J. H. Ormrod, J. R. Macdonald, and H. E. Duckworth, Can. J. Phys. **43**, 275 (1965).
[56] J. E. Valdés, P. Vargas, C. Celedón, E. Sánchez, L. Guillemot, and V. A. Esaulov, Phys. Rev. A **78**, 032902 (2008).
[57] J. Rowe and N. Smith, Phys. Rev. B **10**, 3207 (1974).
[58] N. Smith, G. Wertheim, S. Hüfner, and M. Traum, Phys. Rev. B **10**, 3197 (1974).
[59] D. Roth, D. Goebl, D. Primetzhofer, and P. Bauer, Nucl. Instrum. Method Phys. Res. B **317**, 61 (2013).
[60] O. Grizzi, M. Shi, H. Bu, J. W. Rabalais, and R. A. Baragiola, Phys. Rev. B **41**, 4789 (1990).
[61] V. A. Esaulov, L. Guillemot, and S. Lacombe, Nucl. Instrum. Method Phys. Res. B **90**, 305 (1994).
[62] F. Xu, N. Mandarino, A. Oliva, P. Zoccali, M. Camarca, A. Bonanno, and R. A. Baragiola, Phys. Rev. A **50**, 4040 (1994).
[63] R. Souda, K. Yamamoto, B. Tilley, W. Hayami, T. Aizawa, and Y. Ishizawa, Phys. Rev. B **50**, 18489 (1994).
[64] R. Souda, K. Yamamoto, W. Hayami, T. Aizawa, and Y. Ishizawa, Phys. Rev. B **51**, 4463 (1995).

[65] K. Wittmaack, Surf. Sci. **345**, 110 (1996).
[66] F. Ascione, G. Manico, A. Bonanno, A. Oliva, and F. Xu, Surf. Sci. **394**, L145 (1997).
[67] F. Xu, G. Manicò, F. Ascione, A. Bonanno, A. Oliva, and R. A. Baragiola, Phys. Rev. A **57**, 1096 (1998).
[68] S. Mouhammad, P. Benoit-Cattin, C. Benazeth, P. Cafarelli, P. Reynes, M. Richard-Viard, and J. P. Ziesel, J. Phys.: Condens. Matter **10**, 8629 (1998).
[69] M. Richard-Viard, N. Benazeth, P. Benoit-Cattin, J. P. Ziesel, C. Benazeth, and P. Cafarelli, Nucl. Instrum. Method Phys. Res. B **149**, 7 (1999).
[70] D. Primetzhofer, D. Goebl, and P. Bauer, Nucl. Instrum. Method Phys. Res. B **317**, 8 (2013).
[71] S. Rund, D. Primetzhofer, S. N. Markin, D. Goebl, and P. Bauer, Nucl. Instrum. Method Phys. Res. B **269**, 1171 (2011).
[72] S. Tsuneyuki and M. Tsukada, Phys. Rev. B **34**, 5758 (1986).
[73] N. P. Wang, E. A. García, R. Monreal, F. Flores, E. C. Goldberg, H. H. Brongersma, and P. Bauer, Phys. Rev. A **64**, 012901 (2001).
[74] I. Nagy, I. Aldazabal, and M. L. Glasser, J. Phys. B: At. Mol. Opt. Phys. **45**, 095701 (2012), and references therein.
[75] K. Ladányi, I. Nagy, and B. Apagyi, Phys. Rev. A **45**, 2989 (1992).
[76] D. R. Bates and G. Griffing, Proc. Phys. Soc. London Sect. A **66**, 961 (1953); **67**, 663 (1954).